FERMI DETECTION OF DELAYED GeV EMISSION FROM THE SHORT GAMMA-RAY BURST 081024B

A. A. ABDO[1,2], M. ACKERMANN[3], M. AJELLO[3], K. ASANO[4], W. B. ATWOOD[5], M. AXELSSON[6,7], L. BALDINI[8], J. BALLET[9],
G. BARBIELLINI[10,11], D. BASTIERI[12,13], B. M. BAUGHMAN[14], K. BECHTOL[3], R. BELLAZZINI[8], B. BERENJI[3], P. N. BHAT[15],
E. BISSALDI[16], R. D. BLANDFORD[3], E. D. BLOOM[3], E. BONAMENTE[17,18], A. W. BORGLAND[3], A. BOUVIER[3], J. BREGEON[8], A. BREZ[8],
M. S. BRIGGS[15], M. BRIGIDA[19,20], P. BRUEL[21], J. M. BURGESS[15], T. H. BURNETT[22], S. BUSON[13], G. A. CALIANDRO[23],
R. A. CAMERON[3], P. A. CARAVEO[24], S. CARRIGAN[13], J. M. CASANDJIAN[9], C. CECCHI[17,18], Ö. ÇELIK[25,26,27], V. CHAPLIN[15],
E. CHARLES[3], A. CHEKHTMAN[1,28], J. CHIANG[3], S. CIPRINI[18], R. CLAUS[3], J. COHEN-TANUGI[29], L. R. COMINSKY[30],
V. CONNAUGHTON[15], J. CONRAD[7,31,65], S. CUTINI[32], C. D. DERMER[1], A. DE ANGELIS[33], F. DE PALMA[19,20], S. W. DIGEL[3],
E. DO COUTO E SILVA[3], P. S. DRELL[3], R. DUBOIS[3], D. DUMORA[34,35], C. FARNIER[29], C. FAVUZZI[19,20], S. J. FEGAN[21], G. FISHMAN[36],
W. B. FOCKE[3], P. FORTIN[21], M. FRAILIS[33], Y. FUKAZAWA[37], S. FUNK[3], P. FUSCO[19,20], F. GARGANO[20], D. GASPARRINI[32],
N. GEHRELS[25,38,39], S. GERMANI[17,18], B. GIEBELS[21], N. GIGLIETTO[19,20], P. GIOMMI[32], F. GIORDANO[19,20], T. GLANZMAN[3],
G. GODFREY[3], J. GRANOT[40], I. A. GRENIER[9], M.-H. GRONDIN[34,35], J. E. GROVE[1], L. GUILLEMOT[41], S. GUIRIEC[15], Y. HANABATA[37],
A. K. HARDING[25], M. HAYASHIDA[3], R. H. HAYNES[42], E. HAYS[25], D. HORAN[21], R. E. HUGHES[14], M. S. JACKSON[7,43],
G. JÓHANNESSON[3], A. S. JOHNSON[3], W. N. JOHNSON[1], T. KAMAE[3], H. KATAGIRI[37], J. KATAOKA[44], N. KAWAI[45,46], M. KERR[22],
R. M. KIPPEN[47], J. KNÖDLSEDER[48], D. KOCEVSKI[3], M. L. KOCIAN[3], N. KOMIN[9,29], C. KOUVELIOTOU[36], F. KUEHN[14], M. KUSS[8],
J. LANDE[3], L. LATRONICO[8], M. LEMOINE-GOUMARD[34,35], F. LONGO[10,11], F. LOPARCO[19,20], B. LOTT[34,35], M. N. LOVELLETTE[1],
P. LUBRANO[17,18], G. M. MADEJSKI[3], A. MAKEEV[1,28], M. N. MAZZIOTTA[20], S. McBREEN[16,49], J. E. McENERY[25,39], S. McGLYNN[7,43],
C. MEEGAN[50], P. MÉSZÁROS[38], C. MEURER[7,31], P. F. MICHELSON[3], W. MITTHUMSIRI[3], T. MIZUNO[37], A. A. MOISEEV[26,39],
C. MONTE[19,20], M. E. MONZANI[3], E. MORETTI[10,11], A. MORSELLI[51], I. V. MOSKALENKO[3], S. MURGIA[3], T. NAKAMORI[45],
P. L. NOLAN[3], J. P. NORRIS[52], E. NUSS[29], T. OHNO[53], T. OHSUGI[37], N. OMODEI[8], E. ORLANDO[16], J. F. ORMES[52], W. S. PACIESAS[15],
D. PANEQUE[3], J. H. PANETTA[3], D. PARENT[34,35], V. PELASSA[29], M. PEPE[17,18], M. PESCE-ROLLINS[8], F. PIRON[29], T. A. PORTER[5],
R. PREECE[15], S. RAINÒ[19,20], R. RANDO[12,13], M. RAZZANO[8], S. RAZZAQUE[1,2], A. REIMER[3,54], O. REIMER[3,54], T. REPOSEUR[34,35],
J. RIPKEN[7,31], S. RITZ[5], L. S. ROCHESTER[3], A. Y. RODRIGUEZ[23], M. ROTH[22], F. RYDE[7,43], H. F.-W. SADROZINSKI[5], D. SANCHEZ[21],
A. SANDER[14], P. M. SAZ PARKINSON[5], J. D. SCARGLE[55], T. L. SCHALK[5], C. SGRÒ[8], E. J. SISKIND[56], D. A. SMITH[34,35], P. D. SMITH[14],
G. SPANDRE[8], P. SPINELLI[19,20], M. STAMATIKOS[14,25], M. S. STRICKMAN[1], D. J. SUSON[57], G. TAGLIAFERRI[58], H. TAJIMA[3],
H. TAKAHASHI[37], T. TANAKA[3], J. B. THAYER[3], J. G. THAYER[3], D. J. THOMPSON[25], L. TIBALDO[9,12,13], K. TOMA[38], D. F. TORRES[23,59],
G. TOSTI[17,18], A. TRAMACERE[3,60], E. TROJA[25,45,66], Y. UCHIYAMA[3], T. L. USHER[3], A. J. VAN DER HORST[36,66], V. VASILEIOU[26,27],
N. VILCHEZ[48], V. VITALE[51,61], A. VON KIENLIN[16], A. P. WAITE[3], P. WANG[3], C. WILSON-HODGE[36], B. L. WINER[14], K. S. WOOD[1],
X. F. WU[38,62,63], R. YAMAZAKI[37], T. YLINEN[7,43,64], AND M. ZIEGLER[5]

[1] Space Science Division, Naval Research Laboratory, Washington, DC 20375, USA
[2] National Research Council Research Associate, National Academy of Sciences, Washington, DC 20001, USA
[3] Department of Physics and SLAC National Accelerator Laboratory, W. W. Hansen Experimental Physics Laboratory,
Kavli Institute for Particle Astrophysics and Cosmology, Stanford University, Stanford, CA 94305, USA
[4] Interactive Research Center of Science, Tokyo Institute of Technology, Meguro City, Tokyo 152-8551, Japan; asano@phys.titech.ac.jp
[5] Department of Physics and Department of Astronomy and Astrophysics, Santa Cruz Institute for Particle Physics,
University of California at Santa Cruz, Santa Cruz, CA 95064, USA
[6] Department of Astronomy, Stockholm University, SE-106 91 Stockholm, Sweden
[7] The Oskar Klein Centre for Cosmoparticle Physics, AlbaNova, SE-106 91 Stockholm, Sweden
[8] Istituto Nazionale di Fisica Nucleare, Sezione di Pisa, I-56127 Pisa, Italy; nicola.omodei@gmail.com
[9] Laboratoire AIM, CEA-IRFU/CNRS/Université Paris Diderot, Service d'Astrophysique, CEA Saclay, 91191 Gif sur Yvette, France
[10] Istituto Nazionale di Fisica Nucleare, Sezione di Trieste, I-34127 Trieste, Italy
[11] Dipartimento di Fisica, Università di Trieste, I-34127 Trieste, Italy
[12] Istituto Nazionale di Fisica Nucleare, Sezione di Padova, I-35131 Padova, Italy
[13] Dipartimento di Fisica "G. Galilei," Università di Padova, I-35131 Padova, Italy
[14] Department of Physics, Center for Cosmology and Astro-Particle Physics, The Ohio State University, Columbus, OH 43210, USA
[15] Center for Space Plasma and Aeronomic Research (CSPAR), University of Alabama in Huntsville, Huntsville, AL 35899, USA; narayana.bhat@nasa.gov
[16] Max-Planck Institut für extraterrestrische Physik, 85748 Garching, Germany
[17] Istituto Nazionale di Fisica Nucleare, Sezione di Perugia, I-06123 Perugia, Italy
[18] Dipartimento di Fisica, Università degli Studi di Perugia, I-06123 Perugia, Italy
[19] Dipartimento di Fisica "M. Merlin" dell'Università e del Politecnico di Bari, I-70126 Bari, Italy
[20] Istituto Nazionale di Fisica Nucleare, Sezione di Bari, 70126 Bari, Italy
[21] Laboratoire Leprince-Ringuet, École polytechnique, CNRS/IN2P3, Palaiseau, France
[22] Department of Physics, University of Washington, Seattle, WA 98195-1560, USA
[23] Institut de Ciencies de l'Espai (IEEC-CSIC), Campus UAB, 08193 Barcelona, Spain
[24] INAF-Istituto di Astrofisica Spaziale e Fisica Cosmica, I-20133 Milano, Italy
[25] NASA Goddard Space Flight Center, Greenbelt, MD 20771, USA
[26] Center for Research and Exploration in Space Science and Technology (CRESST) and NASA Goddard Space Flight Center, Greenbelt, MD 20771, USA
[27] Department of Physics and Center for Space Sciences and Technology, University of Maryland Baltimore County, Baltimore, MD 21250, USA
[28] George Mason University, Fairfax, VA 22030, USA
[29] Laboratoire de Physique Théorique et Astroparticules, Université Montpellier 2, CNRS/IN2P3, Montpellier, France
[30] Department of Physics and Astronomy, Sonoma State University, Rohnert Park, CA 94928-3609, USA
[31] Department of Physics, Stockholm University, AlbaNova, SE-106 91 Stockholm, Sweden
[32] Agenzia Spaziale Italiana (ASI) Science Data Center, I-00044 Frascati (Roma), Italy
[33] Dipartimento di Fisica, Università di Udine and Istituto Nazionale di Fisica Nucleare, Sezione di Trieste, Gruppo Collegato di Udine, I-33100 Udine, Italy

[34] Université de Bordeaux, Centre d'Études Nucléaires Bordeaux Gradignan, UMR 5797, Gradignan, 33175, France
[35] CNRS/IN2P3, Centre d'Études Nucléaires Bordeaux Gradignan, UMR 5797, Gradignan, 33175, France
[36] NASA Marshall Space Flight Center, Huntsville, AL 35812, USA
[37] Department of Physical Sciences, Hiroshima University, Higashi-Hiroshima, Hiroshima 739-8526, Japan
[38] Department of Astronomy and Astrophysics, Pennsylvania State University, University Park, PA 16802, USA
[39] Department of Physics and Department of Astronomy, University of Maryland, College Park, MD 20742, USA
[40] Centre for Astrophysics Research, University of Hertfordshire, College Lane, Hatfield AL10 9AB, UK
[41] Max-Planck-Institut für Radioastronomie, Auf dem Hügel 69, 53121 Bonn, Germany
[42] University of Virginia, Charlottesville, VA 22904, USA
[43] Department of Physics, Royal Institute of Technology (KTH), AlbaNova, SE-106 91 Stockholm, Sweden
[44] Waseda University, 1-104 Totsukamachi, Shinjuku-ku, Tokyo, 169-8050, Japan
[45] Department of Physics, Tokyo Institute of Technology, Meguro City, Tokyo 152-8551, Japan
[46] Cosmic Radiation Laboratory, Institute of Physical and Chemical Research (RIKEN), Wako, Saitama 351-0198, Japan
[47] Los Alamos National Laboratory, Los Alamos, NM 87545, USA
[48] Centre d'Étude Spatiale des Rayonnements, CNRS/UPS, BP 44346, F-30128 Toulouse Cedex 4, France
[49] University College Dublin, Belfield, Dublin 4, Republic of Ireland
[50] Universities Space Research Association (USRA), Columbia, MD 21044, USA
[51] Istituto Nazionale di Fisica Nucleare, Sezione di Roma "Tor Vergata," I-00133 Roma, Italy
[52] Department of Physics and Astronomy, University of Denver, Denver, CO 80208, USA
[53] Institute of Space and Astronautical Science, JAXA, 3-1-1 Yoshinodai, Sagamihara, Kanagawa 229-8510, Japan
[54] Institut für Astro- und Teilchenphysik and Institut für Theoretische Physik, Leopold-Franzens-Universität Innsbruck, A-6020 Innsbruck, Austria
[55] Space Sciences Division, NASA Ames Research Center, Moffett Field, CA 94035-1000, USA
[56] NYCB Real-Time Computing Inc., Lattingtown, NY 11560-1025, USA
[57] Department of Chemistry and Physics, Purdue University Calumet, Hammond, IN 46323-2094, USA
[58] INAF Osservatorio Astronomico di Brera, I-23807 Merate, Italy
[59] Institució Catalana de Recerca i Estudis Avançats (ICREA), Barcelona, Spain
[60] Consorzio Interuniversitario per la Fisica Spaziale (CIFS), I-10133 Torino, Italy
[61] Dipartimento di Fisica, Università di Roma "Tor Vergata," I-00133 Roma, Italy
[62] Joint Center for Particle Nuclear Physics and Cosmology (J-CPNPC), Nanjing 210093, China
[63] Purple Mountain Observatory, Chinese Academy of Sciences, Nanjing 210008, China
[64] School of Pure and Applied Natural Sciences, University of Kalmar, SE-391 82 Kalmar, Sweden

ABSTRACT

We report on the detailed analysis of the high-energy extended emission from the short gamma-ray burst (GRB) 081024B detected by the *Fermi Gamma-ray Space Telescope*. Historically, this represents the first clear detection of temporal extended emission from a short GRB. The light curve observed by the *Fermi* Gamma-ray Burst Monitor lasts approximately 0.8 s whereas the emission in the *Fermi* Large Area Telescope lasts for about 3 s. Evidence of longer lasting high-energy emission associated with long bursts has been already reported by previous experiments. Our observations, together with the earlier reported study of the bright short GRB 090510, indicate similarities in the high-energy emission of short and long GRBs and open the path to new interpretations.

Key words: gamma-ray burst: general – gamma-ray burst: individual (GRB 081024B)

Online-only material: color figures

1. INTRODUCTION

Gamma-ray bursts (GRBs) are extremely energetic and brief explosions originating at cosmological distances. Since their discovery in the soft gamma-ray regime roughly 40 years ago, they have been detected to emit in almost every wavelength, from cm to the GeV range. The properties of their gamma-ray emission (e.g., duration, spectral shape, and variability) have been thoroughly studied in the past 20 years with multiple spacecrafts, notably with the Burst And Transient Source Experiment (BATSE) on board the *Compton Gamma Ray Observatory* (*CGRO*; see Zhang & Mészáros 2004 for a review). One of their most enduring properties is their classification into two duration classes (Kouveliotou et al. 1993), with distinct spectral characteristics: short ($\lesssim 2$ s) hard GRBs and long soft ones. This bimodality has been confirmed with NASA's *Swift* satellite (Gehrels et al. 2004) and recently with the Gamma-ray

Burst Monitor (GBM; Meegan et al. 2009) on board the *Fermi* satellite. The prevailing notion is that these two GRB classes originate from different progenitor systems.

The first detection of an X-ray afterglow goes back to observation of GRB 970228 with the *BeppoSAX* satellite (Costa et al. 1997), followed by the discovery of the optical transient (van Paradijs et al. 1997) that allowed the first ever determination of the redshift for a GRB (Bloom et al. 2001). Multi-wavelength (radio to X-ray) follow-up observations of GRB afterglows and the extensive study of the GRB hosts and their environments have now established that at least some long GRBs are connected with the collapse of massive rapidly rotating stars into black holes (Woosley & Bloom 2006, and references therein). The origin of short GRBs is less certain. In the last few years, growing evidence supports the idea that short GRBs originate from neutron star–neutron star mergers also ending in a few solar mass black hole surrounded by a short-lived accretion disk (see Nakar 2007; Eichler et al. 1989; Ruffert & Janka 1999; Rosswog et al. 2000, 2003; Narayan et al. 2001). It is, however, rather difficult observationally to distinguish mergers from collapsars. Supernova explosions have been spectroscopically associated

---

with a scant four cases with GRBs, but none of these have been a short GRB.

The detection of high-energy ($\gtrsim 100$ MeV) prompt and afterglow emission from GRBs with *Fermi* offers a unique probe to test the properties of the outflow, to determine the mechanism of energy transfer, and to address fundamental physics issues like Lorentz invariance, as has been done for other bursts such as GRB 080916C (Abdo et al. 2009c; Zhang & Pe'er 2009) and GRB 090510 (Abdo et al. 2009d). During its first year of operation, *Fermi* detected high-energy photons from two short GRBs (Omodei 2008; Ohno & Pelassa 2009), opening a new window in our understanding of the GRB phenomenon.

High-energy emission above 1 GeV had been detected in the past with *CGRO*/EGRET (Sommer et al. 1994) in association with several long BATSE GRBs. Little was known, however, about the radiation physics of short GRBs, due to poor statistics at higher energies (Kaneko et al. 2006). A notable exception is the extremely bright GRB 930131 (Kouveliotou et al. 1994), which consisted of an initial very intense complex of pulses with total duration about 1.5 s, superimposed on a significant shallow tail lasting up to ∼50 s. As the tail fluence was at least an order of magnitude lower than the one of the initial complex, it was the initial short pulse that dominated the event energetics and most likely contained most of the burst flux. Apart from its intensity, GRB 930131 was also remarkable in its high-energy properties; EGRET detected 16 high-energy gamma rays, including the highest energy photon of 1.2 GeV 26.5 s after the initial spike. As the event was not classified as a short GRB, however, it was not clear until recently that short bursts could produce such high-energy emission, and whether the properties of the short GRB emission resembled those of the long events at GeV energies.

In this paper, we report on the observation and the analysis of the GeV emission from the short GRB 081024B. The event lasts approximately 0.8 s below 5 MeV, entirely consistent with the short GRB class (Kouveliotou et al. 1993). The emission above 100 MeV lasts for about 3 s, thus showing unambiguous evidence for a delayed high-energy component in a short GRB.

2. OBSERVATIONS

The *Fermi Gamma-ray Space Telescope* was launched on 2008 June 11, and during the first year of science operations detected high-energy emission from nine GRBs,[67] doubling the number of bursts detected above 100 MeV. Two instruments operate on board *Fermi*: the Gamma-ray Burst Monitor (GBM; Meegan et al. 2009) covering the energy range from 8 keV to 40 MeV and the Large Area Telescope (LAT; Atwood et al. 2009) from 20 MeV to more than 300 GeV.

On 2008 October 24 at 21:22:41 (UT) the LAT detected an increased count rate associated with the short burst GRB 081024B, which triggered the GBM (trigger number 246576161 (Connaughton & Briggs 2008)). The LAT ground analysis for burst detection and localization follows the procedure described in Abdo et al. (2009b). Selecting "transient" events with energy above 100 MeV, final localization is found to be R.A. = $322°.9$, decl. = $21°.2$, with a statistical uncertainty of $0°.2$ (68% containment radius). The map of the test statistics reaches its maximum value, $TS_{max} = 48.9$, at this position, corresponding to a 6.7σ detection. We also estimated the significance of the high-energy emission using the Li & Ma method (Li & Ma 1983), which computes the probability of the temporal excess in the case of Poisson statistics. We used two different event selections, considering a fixed region of interest (ROI) of $15°$,

and an energy-dependent ROI, taking into account the energy dependence of the LAT point-spread function (PSF). The LAT recorded 11 events with reconstructed energy above 100 MeV, within $15°$ from the position of the burst and within 3 s from the trigger time, when the expected number of counts from the background is 0.75, corresponding to an excess of 6.8σ. The number of expected counts has been computed considering the background 100 s before and 100 s after the burst, excluding the time window of 3 s during the burst. A more careful estimation of the background, using Monte Carlo simulations to estimate the charged particle background, and 6 months of data for estimating the gamma-ray background was also performed, providing a significance of 6.7σ. Details of the method are described in Abdo et al. (2009b). If we consider the energy-dependent ROI, considering only the events that are within 3 times the 68% containment radius of the PSF (approximately corresponding to the 95% of the containment radius), the number of expected events from background decreases to 0.08, and the significance of the excess increases up to 8.5σ. This higher significance can be easily understood as the LAT PSF strongly depends on the energy ($\propto E^{-0.8}$), which makes an energy-dependent ROI very effective in reducing the background contamination, without loosing gamma-ray events from the source.

The LAT position was observed by the Swift X-Ray Telescope (XRT), starting 70.3 ks after the GRB trigger time and lasting 9.9 ks, but no X-ray counterpart was found (Guidorzi et al. 2008). An additional 13.5 ks observation was conducted the next day (Guidorzi & Margutti 2008) and confirmed the lack of an X-ray afterglow candidate. Optical observations also produced no counterpart (Cenko & Kasliwal 2008). The absence of an XRT detection so long after a short burst is not too surprising. A study of the Swift XRT catalog of GRBs[68] shows that of the 33 short GRBs for which XRT observations were made, only 10 had detectable flux 75 ks after the trigger time.

3. LIGHT CURVES, DURATIONS, AND SPECTRAL LAGS

The multi-detector light curve is shown in Figure 1. The top panel shows the background-subtracted light curve for the summed signal of the two brightest NaI detectors (6 and 9) between 8 keV and 260 keV. The background-subtracted light curve of the brightest BGO detector (1) is shown in the second panel (260 keV–5 MeV). The third panel shows the LAT signal without any selection (i.e., all the events that passed the onboard gamma filter). The quality of these events is not good enough to use them in the spectral analysis, but the properties of the ensemble can be assessed quantitatively by means of a dedicated Monte Carlo simulation and do convey physical information in the extremely interesting energy range in which the BGO and the LAT overlap. These three light curves are characterized by a narrow spike of about 0.1 s (interval "a"), followed by a longer pulse, of about 0.7 s (interval "b"). There is no evidence of emission after ∼0.8 s in the NaI and BGO detectors. The bottom panel shows the light curve of the "transient" selected events with well-defined direction and energy (above 100 MeV). The arrival times and the reconstructed energies (right axis) of the selected events are also displayed. We estimate a total of 0.4 background events during the time interval shown in Figure 1. An event with energy 3.1 ± 0.2 GeV was detected after 0.55 s while a second event of 1.7 ± 0.1 GeV was detected after
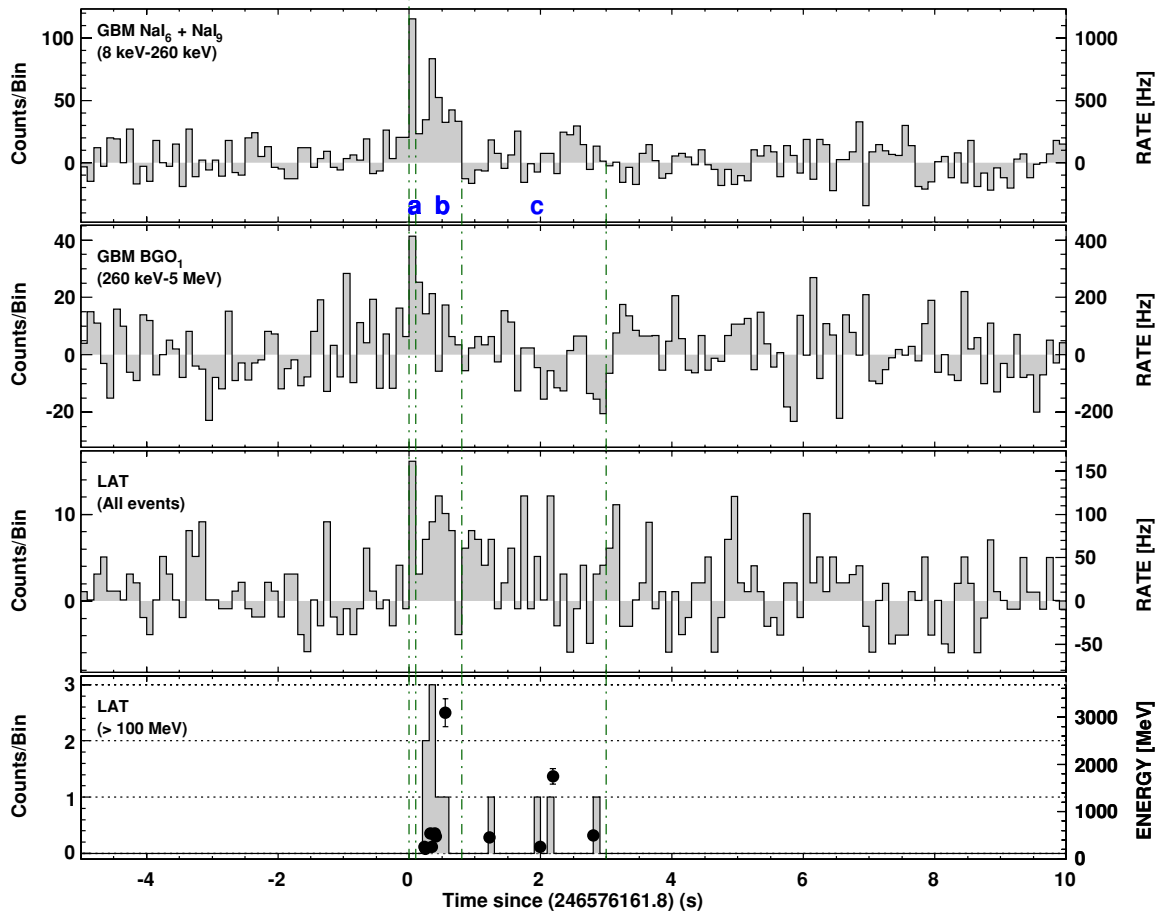
Figure 1. Multi-instrument light curve for GRB 081024B. The top panel shows the sum of the background-subtracted signal from two NaI detectors. The second panel is BGO detector 1. The third panel shows all the events recorded by the LAT, without any selection on the quality of the events (background subtracted). The fourth panel shows the selected "transient" events above 100 MeV. The energy of events is reported at the right axis of the plot. The arrival times, the reconstructed positions, and the energies of the 11 events are reported in Table 1.

(A color version of this figure is available in the online journal.)

Table 1
Selected LAT "Transient" Events with Energy Above 100 MeV

	Time-$T_{\rm trig}$[a] (s)	Energy[b] (MeV)	R.A. (deg)	Decl. (deg)	PSF[c] (deg)	Dist.[d] in PSF
1	0.229	145 ± 22	325.3	21.4	2.6	0.8
2	0.248	101 ± 17	323.2	18.7	3.4	0.7
3	0.320	442 ± 44	322.6	20.6	1.1	0.6
4	0.342	140 ± 21	322.2	20.2	2.7	0.4
5	0.391	441 ± 44	323.6	20.9	1.1	0.7
6	0.406	368 ± 41	323.1	18.8	1.2	1.2
7	**0.551**	**3070 ± 230**	**322.9**	**21.2**	**0.2**	**0.2**
8	1.223	350 ± 39	324.1	20.7	1.3	1.0
9	1.986	143 ± 22	325.0	24.2	2.6	1.4
10	**2.184**	**1680 ± 130**	**322.7**	**21.5**	**0.4**	**1.0**
11	2.801	386 ± 41	322.6	20.1	1.2	1.0

Notes. Bold values are relative to the two events with highest energies, greater than 1 GeV.
[a] Arrival time with respect to the GBM trigger time $T_{\rm trig} = 246576161.864$.
[b] Reconstructed energy with estimated error. Errors are estimated using Monte Carlo simulations from the width of the reconstructed energy distribution.
[c] Evaluated 68% containment radius from the PSF for "transient" events.
[d] Distance from the GRB position, in PSF units.

2.18 s. Table 1 contains the arrival times, the energies with the estimated error, and the arrival directions of these 11 selected events. The last two columns of the table are the estimated 68% containment radii calculated from the PSF and the distance from the localization of the GRB, in PSF units.

We studied the narrow spike visible in the full light curve (third panel) of interval "a." The probability to obtain the same number of counts from background fluctuations is discarded at the 3.5σ level. Furthermore, we performed dedicated Monte Carlo simulations to estimate properly the energy of these LAT photons. These events do not belong to the "transient" class, which is the most generous event selection with minimal requirements on direction and energy reconstructions. Typically, they are discarded because they produce very few hits in the tracker (<20), with a very short track, and very low raw energy deposited in the calorimeter (<5 MeV). These topologies are typical of low-energy events, with energies between 10 MeV and 40 MeV. If we select these topologies in the data, the probability that this narrow pulse is the result of a background fluctuation decreases to 5.9σ level.

We conclude that the spike in interval "a" in the LAT data is *significant*, with energies below 100 MeV (although the energy resolution for this class of events is relatively poor, ∼50%, from Monte Carlo simulations).

A common method for estimating GRB durations is to compute the T_{90} which measures the duration of the time interval during which 90% of the total observed counts have been

Table 2
Fit Parameters for the Time-resolved Spectral Fits

Fit	Interval (s)	Detectors	Model	E_{peak} (MeV)	α	β	C-Stat/DOF	Fluence (20 keV–2 MeV) (erg cm^{-2})	Fluence (100 MeV–10 GeV) (erg cm^{-2})
1	"a," 0–0.1	NaI+BGO	COMPT	$2.7^{+4.3}_{-1.5}$	$-1.03^{+0.23}_{-0.19}$	$\cdots$	330/352	$(1.7 \pm 0.3) \times 10^{-7}$	$< 4.7 \times 10^{-10}$
2	"a," 0–0.1	NaI+BGO	BAND	$2.8^{+5.0}_{-1.5}$	$-1.03^{+0.23}_{-0.20}$	$< -1.7^{\text{a}}$	330/351	$(1.7 \pm 0.4) \times 10^{-7}$	$< 7.3 \times 10^{-8}$
3	"b," 0.1–0.8	NaI+BGO+LAT	BAND	$2.0^{+1.9}_{-1.0}$	$-1.03^{+0.17}_{-0.14}$	$-2.10^{+0.11}_{-0.14}$	383/359	$(7.9 \pm 1.9) \times 10^{-7}$	$(8.9 \pm 3.0) \times 10^{-7}$
4	"b," 0.1–0.8	NaI+BGO+LAT	COMPT + POW	$1.6^{+1.5}_{-0.6}$ $\cdots$	$-0.7^{+0.4}_{-0.3}$ $\cdots$	$\cdots$ $-1.68^{+0.10}_{-0.06}$	384/358	$(8.8 \pm 2.0) \times 10^{-7}$	$(1.1 \pm 0.4) \times 10^{-6}$
5	"c," 0.8–2.9	NaI+BGO+LAT	POW	$\cdots$	$\cdots$	$-1.6^{+0.4}_{-0.1}$	274/361	$(4.3 \pm 3.2) \times 10^{-8}$	$(4.0 \pm 2.4) \times 10^{-7}$

Notes. For each time bin ("a," "b," and "c"), and for each fit (1–5), we report the detectors used in the fit, the name of the model used, and the value of each spectral parameter. Asymmetric errors are obtained from the profile of the Cash statistic. The pivot energy of the power-law function is set to 100 MeV.
[a] The upper limit for β has been obtained looking at the profile of the Cash statistic. Although in this fit β is basically undetermined, we report it for reference.

detected (Kouveliotou et al. 1993). Background fluctuations, especially in weak GRBs, strongly affect T_{90}s as often the fluctuations are comparable to the 5% of the total GRB fluence. Values of T_{50}, however, are generally more robust, and especially so in the case of weak events. For GRB 081024B, the T_{50} (T_{90}) is 0.33 s (0.66 s) in the NaI detectors, 0.15 s (0.27 s) in the BGO, while it is significantly longer for the LAT, corresponding to 0.9 s (2.1 s) for the full statistic light curve and 1.5 s (2.6 s) selecting only the events above 100 MeV.

Spectral lags are characteristic of long GRBs, which exhibit hard-to-soft spectral evolution, while short GRBs do not exhibit such a property (Norris & Bonnell 2006). We searched for a possible spectral lag in GRB 081024B using the cross-correlation function (CCF). The GBM time tagged event light curves of the four brightest NaI detectors (6, 7, 9, and 10) were summed with 100 ms time resolution in eight logarithmic energy bins from 8 to 1950 keV. Similarly, the two BGO light curves were added in eight bins from 0.11 to 107.6 MeV. For the LAT, we used all photons above 100 MeV. The errors on the CCFs were estimated using Bartlett's formula (Bartlett 1978) and were propagated to the errors of the peak position. We computed the CCFs between the GBM/NaI and the GBM/BGO detectors as well as between the GBM and the LAT. We found no energy-dependent delay between any of the data types used. We also used two resolutions (50 and 100 ms) and verified that our results did not change significantly.

4. SPECTRAL ANALYSIS

We performed a time-resolved spectral analysis in intervals "a," "b," and "c" of Figure 1, simultaneously fitting the signal from the two NaI (selecting all the channels between 8 keV and 860 keV), the BGO (from 200 keV to 36 MeV), and the LAT detectors (selecting "transient" events above 100 MeV).[69] Table 2 shows the results for all time intervals, testing different fitting functions.

In interval "a" the best fit to the GBM data is obtained with a power law with exponential cutoff (Kaneko et al. 2006, see COMPT model). The best-fit parameters are summarized in Table 2 as fit "1." The peak energy E_{peak} lies in the BGO energy range, and, even though its value is only marginally constrained, is consistent with a very hard spectrum, with a roll-off at energies above a few MeV. The LAT upper limit on the photon flux in the

100 MeV–10 GeV energy range is 3.8×10^{-5} photons cm^{-2} s^{-1} or, in energy flux, 4.7×10^{-9} erg cm^{-2} s^{-1}, and is consistent with the extrapolated flux from the COMPT function fitted to the GBM data. We also performed a fit using the Band function (Band et al. 1993). The resulting parameters are listed in Table 2 as fit "2."

Interval "b" is best represented by a Band function with the parameters displayed in Table 2 as fit "3." To estimate the significance of the spectral evolution from interval "a" to interval "b" we fit the count spectrum in interval "a" assuming a Band function with a fixed high-energy spectral index obtained by the best fit of interval "b" ($\beta = -2.1$), and we estimate the number of expected events in the LAT detector. Based on several realizations, the average number of expected events in interval "a" is 2.6, for a chance probability of observing zero counts of about 7%. Therefore, we can only suggest that a spectral evolution characterizes the temporal behavior of this burst, somewhat similar to that observed in the first portion of the emission of the long, bright GRB 080916C (Abdo et al. 2009c). Fit "4" shows the result of the fit when a COMPT model plus a power law is adopted. Even though the fit is not favored, and the statistics are very low for any conclusive remark, this model has some interesting implications, such as the possible presence of an extra component in LAT data.

The last entry in the table is related to interval "c" which is best represented by a simple power law. Figure 2 shows the count spectrum for the fit "3" and Figure 3 the stacked νF_ν plot for fits 1, 3, 4, and 5, where the 68% CL are computed from the covariance matrix provided by the fitting routine (*rmfit*).

Systematic errors are due to uncertainties in the effective areas of the different detectors, energy resolution, and background estimation. The most important contribution arises from the uncertainties related to the effective areas. For the LAT, they have been derived from a study of the Vela pulsar (Abdo et al. 2009a) and are 10% below 100 MeV, 5% around 1 GeV and 20% above 10 GeV. We adopt a 10% uncertainty in the NaI and BGO effective area (both overall normalization and slope). We propagate the systematic errors on the effective areas to the parameters of the model, and we compute the systematic errors associated with the flux/fluence values. Systematic errors in each case are comparable or smaller than the statistical errors quoted in Table 2.

5. DISCUSSION AND INTERPRETATION

GRB 081024B was the first short GRB with observed emission above GeV energies. Unlike GRB 930131 (Kouveliotou

---

[69] Here, we have used the post-launch Pass 6 v3 IRFs, which take into account, on average, the correction of the inefficiency due to pile-up of cosmic rays. The version of Science Tools used is v15r9p2. We have used the package *rmfit* (version 3.1) to perform the GBM/LAT joint fit.
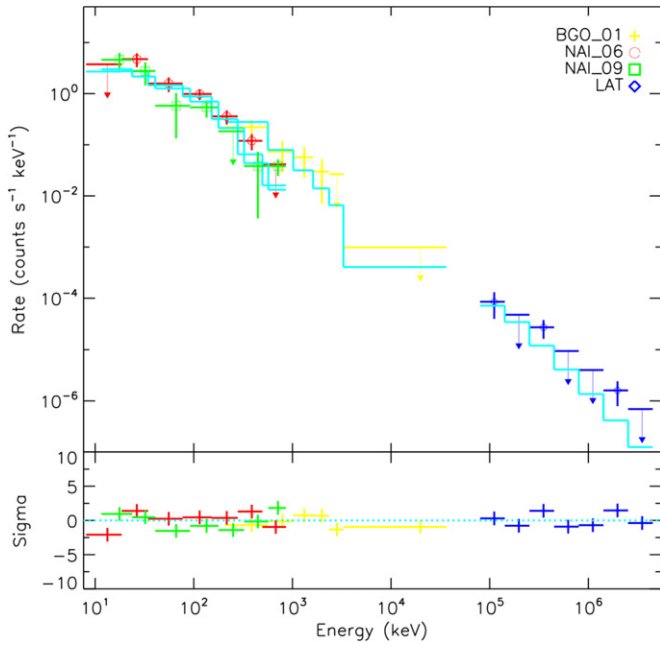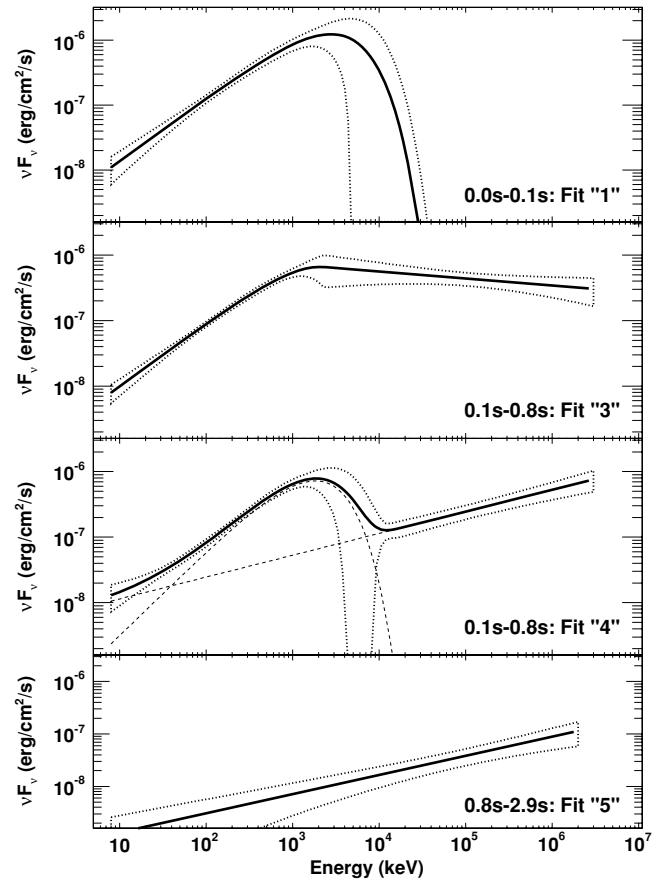
Figure 2. Count spectrum in interval "b," fit "3." The data points are the rates from GBM (red circles: NaI_6; green squares: NaI_9; and yellow crosses: BGO_1) and LAT (blue diamonds). The predicted rates in the various detectors are obtained by folding the best-fit model (Band function) with the response of the detectors, and are displayed as continuous cyan lines.

(A color version of this figure is available in the online journal.)

Figure 3. Analytical representation of the source photon spectra. From top to bottom: fit "1" in interval "a" (COMPT model); fit "3" in interval "b" (Band); fit "4" in interval "b" (COMPT plus power law); and fit "5" in interval "c" (power law).

Figure 4. Fluence–fluence diagram for six LAT GRBs. Black squares are classified as short GRBs and filled gray circles represent long GRBs. The dashed lines indicate the 1, 0.1, and 0.01 values of the ratios between the 100 MeV–10 GeV fluence and the 20 keV–2 MeV fluence.

et al. 1994; Sommer et al. 1994), a 3 GeV photon from GRB 081024B is well correlated with the second low-energy pulse. The CCF of the light curves between 30–100 keV and 100–300 keV shows no strong signature of spectral lag larger than 30 ms, which is consistent with the negligible spectral lags in other short GRBs (Norris & Bonnell 2006).

While the majority of long GRB spectra are well fitted by the conventional Band function, previous spectral analyses of short GRBs have mostly used the cutoff power-law function (Ghirlanda et al. 2004; Mazets et al. 2004). The exponential cutoff implies that the bulk motion of short GRBs is not necessarily ultrarelativistic, owing to the compactness problem for high-energy photons above $m_e c^2$ (Meszaros 2002), which becomes less severe (see, Nakar 2007) for a quantitative estimate of the Γ_{min} in this case). This difference between long and short GRBs may be due to poor counting statistics at high energies in short GRBs, stressing the need for a larger sample with sufficient high-energy photons in MeV–GeV bands.

The delayed onset of a GeV pulse, which is frequently found in other LAT-detected bursts such as GRB 080916C or GRB 090902B, may be explained by the different physical parameters for two pulses (Abdo et al. 2009c), $\gamma\gamma$ pair-production opacity effect (Granot et al. 2008), or acceleration timescale of high-energy protons for hadronic models (e.g., Rachen & Meszaros 1998; Dermer 2002; Razzaque et al. 2005; Dermer & Atoyan 2006; Asano & Inoue 2007; Asano et al. 2009). The long-lasting tail of GeV emission is also common to GRB 080916C, GRB 080825C, and GRB 090510. One possible interpretation is that the long tail is synchrotron or synchrotron self-Compton (SSC) emission during the afterglow phase (Ghirlanda et al. 2009). Alternatively, the GeV afterglow emission may originate from cascades induced by ultrarelativistic hadrons accelerated by the blast wave (Bottcher & Dermer 1998). In these afterglow scenarios even the 3 GeV photon at
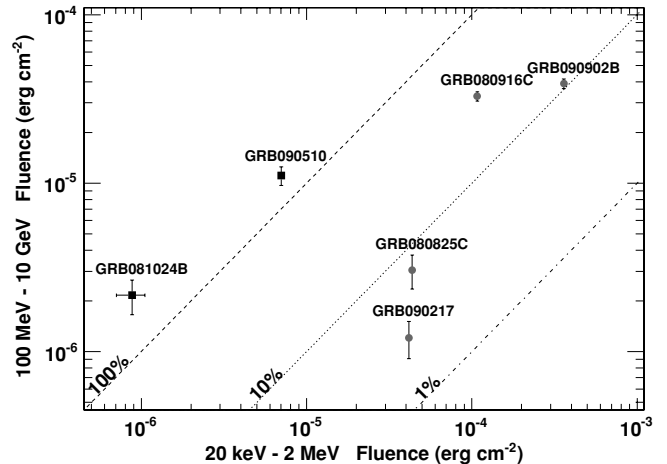
$t \simeq 0.5$ s could have an afterglow origin, and the delayed onset of GeV emission is also naturally explained. The onset time (Molinari et al. 2007) and the hard spectrum for interval "c" do not contradict the afterglow scenarios. Early afterglow models for this long-lasting tail with synchrotron emission (He & Wang 2009) and SSC emission (Corsi et al. 2009) are actually proposed. On the other hand, Corsi et al. (2009) pointed out that

SSC emission from late internal shocks can be an alternative interpretation for the long-lasting tail.

Finally, in Figure 4 we show the high-energy fluence versus low-energy fluence diagram, as suggested by (Le & Dermer 2009), comparing six LAT GRBs. This is considered as a way to search for separate classes of GRBs and, specifically, spectral differences between the short-hard and long duration GRB classes. The sample is limited and therefore no definite conclusion can be drawn, but we note that the two short bursts so far detected by the LAT occupy a region where the energy emitted at high energy is greater than the energy emitted at lower energy (with a ratio $\gtrsim 1$) suggesting that short GRBs may have a higher efficiency in emitting γ-rays. Nowadays only two short GRBs have been detected with a significant emission at GeV energies; we expect that in the next decade we will be able to significantly increase the *Fermi* short GRB sample and understand their similarities and differences from the long, soft GRBs.

REFERENCES

Abdo, et al. 2009a, ApJ, 696, 1084
Abdo, et al. 2009b, ApJ, 707, 580
Abdo, et al. 2009c, Science, 323, 1688
Abdo, et al. 2009d, Nature, 462, 331
Asano, K., & Inoue, S. 2007, ApJ, 671, 645
Asano, K., Inoue, S., & Mészáros, P. 2009, ApJ, 699, 953
Atwood, et al. 2009, ApJ, 697, 1071
Band, et al. 1993, ApJ, 413, 281
Bartlett, M. 1978, An Introduction to Stochastic Processes (Cambridge: Cambridge Univ. Press)
Bloom, J. S., Djorgovski, S. G., & Kulkarni, S. R. 2001, ApJ, 554, 678

Bottcher, M., & Dermer, C. 1998, ApJ, 499, L131
Cenko, S. B., & Kasliwal, M. M. 2008, GRB Coordinates Network, 8417, 1
Connaughton, V., & Briggs, M. 2008, GRB Coordinates Network, 8408, 1
Corsi, A., Guetta, D., & Piro, L. 2009, A&A, submitted (arXiv:0905.1513)
Costa, E., et al. 1997, Nature, 387, 783
Dermer, C. 2002, ApJ, 574, 65
Dermer, C., & Atoyan, A. 2006, New J. Phys., 8, 122
Eichler, D., Livio, M., Piran, T., & Schramm, D. N. 1989, Nature, 340, 126
Gehrels, N., et al. 2004, ApJ, 611, 1005
Ghirlanda, G., Ghisellini, G., & Celotti, A. 2004, A&A, 422, L55
Ghirlanda, G., Ghisellini, G., & Nava, L. 2009, ApJ, submitted (arXiv:0909.0016)
Granot, J., Cohen-Tanugi, J., & do Couto e Silva, E. 2008, ApJ, 677, 92
Guidorzi, C., & Margutti, R. 2008, GRB Coordinates Network, 8416, 1
Guidorzi, C., Margutti, R., & Mao, J. 2008, GRB Coordinates Network, 8410, 1
He, H.-N., & Wang, X.-Y. 2009, Science in China Ser. G, submitted (arXiv:0908.2580)
Kaneko, Y., Preece, R. D., Briggs, M. S., Paciesas, W. S., Meegan, C. A., & Band, D. L. 2006, ApJS, 166, 298
Kouveliotou, C., Meegan, C. A., Fishman, G. J., Bhat, N. P., Briggs, M. S., Koshut, T. M., Paciesas, W. S., & Pendleton, G. N. 1993, ApJ, 413, L101
Kouveliotou, C., et al. 1994, ApJ, 422, L59
Le, T., & Dermer, C. D. 2009, ApJ, 700, 1026
Li, T.-P., & Ma, Y.-Q. 1983, ApJ, 272, 317
Mazets, E., Aptekar, R., Frederiks, D., Golenetskii, S., Il inskii, V., Palshin, V., Cline, T., & Butterworth, P. 2004, in ASP Conf. Ser. 312 Third Rome Workshop on Gamma-ray Bursts in the Afterglow Era, ed. M. Feroci et al. (San Francisco, CA: ASP), 102
Meegan, C., et al. 2009, ApJ, 702, 791
Meszaros, P. 2002, ARA&A, 40, 137
Molinari, E., et al. 2007, A&A, 469, 13
Nakar, E. 2007, Phys. Rep., 442, 166
Narayan, R., Piran, T., & Kumar, P. 2001, ApJ, 557, 949
Norris, J., & Bonnell, J. 2006, ApJ, 643, 266
Ohno, M., & Pelassa, V. 2009, GRB Coordinates Network, 9334, 1
Omodei, N. 2008, GRB Coordinates Network, 8407, 1
Rachen, J., & Meszaros, P. 1998, Phys. Rev. D, 58, 123005
Razzaque, S., Mészáros, P., & Waxman, E. 2005, Int. J. Mod. Phys. A, 20, 3099
Rosswog, S., Davies, M. B., Thielemann, F.-K., & Piran, T. 2000, A&A, 360, 171
Rosswog, S., Ramirez-Ruiz, E., & Davies, M. B. 2003, MNRAS, 345, 1077
Ruffert, M., & Janka, H.-T. 1999, A&A, 344, 573
Sommer, M., et al. 1994, ApJ, 422, L63
van Paradijs, J., et al. 1997, Nature, 386, 686
Woosley, S. E., & Bloom, J. S. 2006, ARA&A, 44, 507
Zhang, B., & Mészáros, P. 2004, Int. J. Mod. Phys. A, 19, 2385
Zhang, B., & Pe'er, A. 2009, ApJ, 700, L65